

Photochemical Properties of Excited Triplet State of 6*H*-Purine-6-thione Investigated by Laser Flash Photolysis

Maksudul M. Alam, Mamoru Fujitsuka, Akira Watanabe, and Osamu Ito*

Institute for Chemical Reaction Science, Tohoku University, Katahira, Aoba-ku, Sendai, 980-77, Japan

Received: October 8, 1997; In Final Form: December 10, 1997

Photochemical reactions of 6*H*-purine-6-thione (PuT) via the excited triplet state [³(PuT)*] have been studied by means of laser flash photolysis in organic solvents. Transient absorption bands at 475 and 690 nm were assigned to ³(PuT)*. Intersystem quantum yield and the lowest triplet energy of ³(PuT)* were evaluated to be 0.99 and 63 kcal/mol, respectively. The self-quenching rate constant is quite large ($2.3 \times 10^9 \text{ M}^{-1} \text{ s}^{-1}$ in THF). In photoinduced electron transfer, ³(PuT)* acts as electron acceptor for tetramethylbenzidine, while ³(PuT)* acts as electron donor for *p*-dinitrobenzene. Rate constants for H-atom abstraction (k_{HT}) of ³(PuT)* from benzenethiols, tocopherol, and 1,4-cyclohexadiene are on the order of $10^8 \text{ M}^{-1} \text{ s}^{-1}$. From the Hammett plots of k_{HT} for substituted benzenethiols, a negative ρ value indicates that ³(PuT)* has electrophilic character. In the addition reaction of ³(PuT)* toward various alkenes, the electrophilic character of ³(PuT)* was also confirmed. By steady-light photolysis of PuT, purine was produced via ³(PuT)* after H-atom abstraction. On combination of these results, the character of the lowest ³(PuT)* was presumed.

Introduction

The photochemistry of aliphatic thiones and aromatic thiones has been well studied;^{1–6} the importance of the triplet states of thiones has been revealed in the photochemical reactions.^{7,8} In the case of N-atom-containing thiones, however, the photochemical properties have not been studied compared with thiones without N atoms; i.e., even in various recent reviews about the photoexcited thiones, the descriptions of the thiones with N atoms are excluded because of lack of the systematic studies.^{9,10}

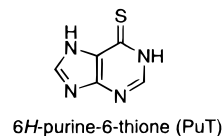
The photochemistry of thiones with N atoms is important in chemical viewpoints^{11,12} and biological viewpoints.^{13–15} Chemically, various interesting photochemical reactions are known especially for pyridine thiones.^{11,12} Biochemically, photolysis of these thiones was used for specific fission of DNA sequence. For example, 6*H*-purine-6-thione (PuT in Scheme 1) can photosensitize the destruction of free-radical-scavenging antioxidants, thereby depleting the system of its biological defenses.¹⁵ Hemmens and Moore reported that photoionization in aqueous solution is strongly related to biological activities.^{15,16} Thus, it is important to investigate the photochemical reactivities of PuT in more detail in organic solvents.

In the present paper, we report photochemical behavior such as energy transfer, electron transfer, H-atom abstraction, and addition reaction toward alkenes of the triplet state of PuT [³(PuT)*] measured mainly by nano-second laser flash photolysis. By prolonged steady-light illumination, the photochemical reaction of PuT was also observed in organic solvents with H-atom donor ability.

Experimental Section

Materials and Steady-State Measurements. PuT was obtained from Aldrich Chemical Co. in a purity of >99%. 3,3',5,5'-Tetramethylbenzidine (TMB), *p*-dinitrobenzene (DNB), and other aromatic hydrocarbons were purified by recrystalli-

SCHEME 1



zation. Commercially available dienes were purified by distillation. Solvents were of spectroscopic grade.

Steady-state photolysis was performed with light of wavelength longer than 310 nm from Xe–Hg lamp (150 W). The photodesulfurization reaction of PuT yielding purine was confirmed by the characteristic UV band and the GC–MS peak of purine. Formation of H₂S was confirmed by its reduction ability from CuSO₄ to CuS. The quantum yield of the photochemical reaction was evaluated by the actinometric method using potassium ferric oxalate.¹⁷ Absorption spectra of the radical ions of PuT were measured by γ irradiation in frozen glassy Me–THF solution at 77 K. The phosphorescence spectrum was measured at 77 K in glassy Me–THF.

Transient Absorption Measurements. The nanosecond time-scale laser photolysis apparatus was a standard design with a Nd:YAG laser (6 ns fwhm).^{18,19} Transient spectra were recorded with a multichannel photodiode (MCPD) system in the visible region by photolysis of PuT with third-harmonic-generated (THG) light (355 nm). The time profiles were followed by a photomultiplier tube (PMT) in the visible region. In the near-IR region, a Ge APD (germanium avalanche photodiode) module was employed, using a pulsed Xe lamp (60 μs fwhm). Picosecond laser photolysis was performed with a mode-locked Nd:YAG laser (35 ps duration). The transient absorption spectra were observed by monitoring light from Xe breakdown with a streak camera detector.^{20,21} Laser photolysis was performed for deaerated solutions obtained by Ar-bubbling in a rectangular quartz cell with a 10-mm optical path at 23 °C.

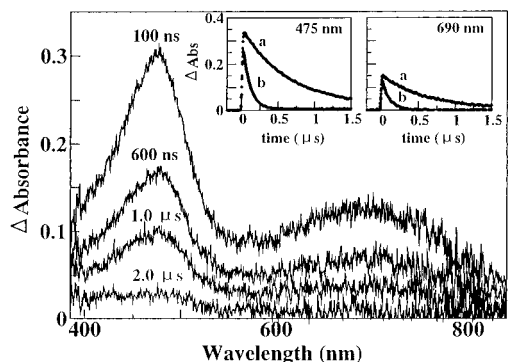
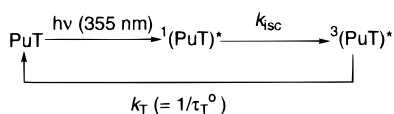


Figure 1. Transient absorption spectra observed after laser photolysis of PuT (0.5 mM) with 355-nm light (detector, MCPD) in Ar-saturated THF. Inset shows time profiles of absorption bands: (a) in Ar-saturated and (b) aerated solution (detector, PMT).

SCHEME 2



Results and Discussion

Ground-State Absorption of PuT. The UV–visible absorption spectrum of PuT shows the absorption peak at 331 nm with high molar extinction coefficient ($\epsilon = 18\,000 \text{ M}^{-1} \text{ cm}^{-1}$), suggesting that the 331-nm band has the π – π^* character. At higher concentration, a very weak band with fine structure was observed at ca. 430 nm with $\epsilon = 20$ – $30 \text{ M}^{-1} \text{ cm}^{-1}$, which can be ascribed to the forbidden n – π^* transition. These spectral features are similar to those of aliphatic and aromatic thiones without N atoms except that the n – π^* transition of PuT is extremely low in intensity and close to the π – π^* transition.^{4,6,10}

No fluorescence was observed at room temperature for PuT. This suggests that the properties of the excited singlet states of PuT are quite different from those of thiones without N atoms, for which intense fluorescence from the second-excited singlet state was reported.^{4,6,22}

The spectral shape of the dilute PuT solution (0.1 mM) is the same as that of the concentrated solution (up to 0.5 mM). The absorption intensities show a linear increase with the concentration, indicating that aggregation of PuT may not be appreciable in the concentration range up to ca. 0.5 mM.

Laser Flash Photolysis. The transient absorption spectra observed by the laser photolysis of PuT in Ar-saturated THF with 355-nm light exhibit an absorption band at 475 nm in addition to a weak band around 690 nm as shown in Figure 1. The absorption intensities of both bands, which decrease within a few microseconds in THF, were quenched very quickly in the presence of oxygen (inset in Figure 1) and other triplet quenchers, suggesting that both 475 and 690 nm absorptions were due to ${}^3(\text{PuT})^*$ (Scheme 2).

The 690-nm band was not effectively scavenged by solvated electron quenchers such as *m*-terphenyl,²³ indicating that the 690-nm peak was the absorption band of ${}^3(\text{PuT})^*$ but not the absorption band of the solvated electron. By excitation of PuT in aqueous solution with the 266-nm light, the broad absorption band was observed at ca. 520 nm, which can be attributed to the solvated electron formed by photoionization.^{15,16}

The rate constant of the intersystem-crossing process of PuT (k_{isc}) was measured by the picosecond laser-photolysis method because of its absence of fluorescence.²² The transient absorption band of ${}^3(\text{PuT})^*$ was observed immediately after the 35-

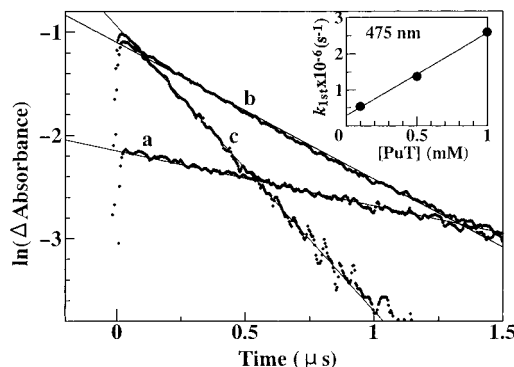


Figure 2. Concentration dependence of first-order plots for decay of ${}^3(\text{PuT})^*$ at 475 nm in Ar-saturated THF (detector, PMT); [${}^3(\text{PuT})^*$] (a) 0.1, (b) 0.5 and (c) 1.0 mM. Inset shows pseudo-first-order plot.

TABLE 1: Absorption Maximum (λ_{max}), Viscosity (η), Intrinsic Triplet Lifetime (τ_{T}°), and Self-Quenching Rate Constant (k_{sq}) of ${}^3(\text{PuT})^*$ in Various Solvents

solvents	$\lambda_{\text{max}}/\text{nm}^a$	$\tau_{\text{T}}^{\circ}/\mu\text{s}^b$	$k_{\text{sq}}/\text{M}^{-1} \text{ s}^{-1}^b$	η/cP
THF	476 ^c	3.53	2.3×10^9	0.55
2-PrOH	471	2.16	8.6×10^8	2.86
ethanol	470	5.33	1.7×10^9	1.08
acetonitrile	469	4.48	4.9×10^9	0.35

^a Each λ_{max} value contains estimation error of $\pm 1 \text{ nm}$. ^b Infinite lifetime (τ_{T}°) was estimated by the extrapolation to infinite dilution in the plots of $k_{\text{obs}}(1/\tau_{\text{T}})$ vs [PuT]; k_{sq} was evaluated from the slope. ^c The ϵ_{T} value in THF was estimated to be $6100 \text{ M}^{-1} \text{ cm}^{-1}$ for ${}^3(\text{PuT})^*$ at 475 nm.

laser excitation at 355 nm. From the time profile of the rise of ${}^3(\text{PuT})^*$, the k_{isc} value can be evaluated to be $> 1.3 \times 10^{10} \text{ s}^{-1}$.

Self-Quenching of ${}^3(\text{PuT})^*$. It is reported that self-quenching reaction 1 is one of the characteristics of the excited triplet states of thiones.⁴



The triplet-decay lifetimes (τ_{T}) of ${}^3(\text{PuT})^*$ were measured as a function of ground-state PuT concentration in the limit of the low laser powers (2.0–5.0 mJ/pulse) as shown in Figure 2.

For the decay of ${}^3(\text{PuT})^*$, the first-order rate constant ($k_{\text{T}} = 1/\tau_{\text{T}}$) increases with [PuT]. The self-quenching rate constant (k_{sq}) and the triplet lifetime (τ_{T}°), which are defined as intrinsic in each solvent, can be evaluated from eq 2:³

$$1/\tau_{\text{T}} = 1/\tau_{\text{T}}^{\circ} + k_{\text{sq}}[\text{PuT}] \quad (2)$$

Similarly, high self-quenching ability [$k_{\text{sq}} = (0.8$ – $5) \times 10^9 \text{ M}^{-1} \text{ s}^{-1}$] was observed for ${}^3(\text{PuT})^*$ in various solvents (Table 1). The k_{sq} values seem to depend on the viscosity of the solvent, suggesting that they are close to the diffusion-controlled limit. These k_{sq} values are similar to those reported for xanthione triplet state in perfluoroalkane solvent.⁵

The τ_{T}° values are smaller than those of aromatic carbonyl compounds. Small τ_{T}° values are one of the characteristics of the thiones, which may be caused by rapid T_1 – S_1 equilibrium of PuT in addition to the spin–orbit coupling of the S atom. The τ_{T}° value for ${}^3(\text{PuT})^*$ in 2-propanol (2-PrOH) is slightly smaller than those in other solvents. Since τ_{T}° was defined in each solvent, the observed short τ_{T}° value may be related to the H-abstraction reaction of ${}^3(\text{PuT})^*$ from 2-PrOH.

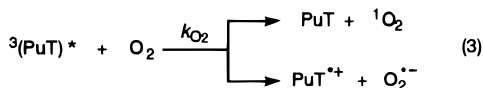
In the presence of well-known triplet quenchers such as O_2 , the decay rates of the transient absorption bands at 475 and 690 nm increase as shown in Figure 1. From these decay rates,

TABLE 2: Rate Constants for Reactions of $^3(\text{PuT})^*$ with Triplet Quenchers and Reactants at 23 °C in THF

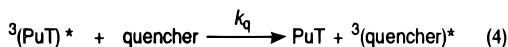
quenchers	$E_{T_1}/\text{kcal M}^{-1}$	$k_q/\text{M}^{-1} \text{s}^{-1}$ ^a	reaction type
β -carotene	19.4 ^b	9.7×10^{10}	T-energy transfer
O ₂	22.5 ^c	4.6×10^9	T-energy transfer
ferrocene	42.9 ^d	7.1×10^9	T-energy transfer
1,3-CHD ^g	52.4 ^c	6.3×10^9	T-energy transfer
isoprene	60.1 ^c	4.1×10^9	T-energy transfer
phenanthrene	62.0 ^c	3.5×10^9	T-energy transfer
<i>m</i> -terphenyl	64.3 ^c	2.4×10^7	T-energy transfer
diphenyl	65.8 ^c	5.8×10^5	T-energy transfer
1,4-CHD ^g	78.0 ^e	6.6×10^7 ^f	H-abstraction

^a Estimation error is $\pm 5\%$. ^b Reference 25. ^c Reference 27. ^d Reference 26. ^e Reference 28. ^f Rate constant is due to H-atom abstraction (k_{HT}). ^g CHD: cyclohexadiene.

the second-order triplet-quenching rate constant (k_{O_2} in reaction 3) was evaluated to be $6.4 \times 10^9 \text{ M}^{-1} \text{ s}^{-1}$ for O₂ in THF. In our study, the formation of singlet O₂ was confirmed by consumption of 1,3-diphenylisobenzofuran.²⁴ Hemmens et al. reported that both ¹O₂ and superoxide (O₂^{•-}) are formed by the laser flash photolysis of PuT in aqueous solution. Formation of O₂^{•-} is possible via electron transfer from PuT to ¹O₂ in aqueous solution.¹⁵



For other triplet quenchers (reaction 4),^{25–28} the k_q values thus obtained are summarized in Table 2. Although the k_q value for phenanthrene ($3.5 \times 10^9 \text{ M}^{-1} \text{ s}^{-1}$; $E_{T_1} = 62.0 \text{ kcal/mol}$)²⁷ is still close to the diffusion-controlled limit, the k_q value for *m*-terphenyl ($2.4 \times 10^7 \text{ M}^{-1} \text{ s}^{-1}$; $E_{T_1} = 64.3 \text{ kcal/mol}$)²⁷ is about 1/100 of the diffusion limit, indicating that E_{T_1} of $^3(\text{PuT})^*$ is close to 62.5 kcal/mol as calculated from the Sandros equation:²⁹



The E_{T_1} of $^3(\text{PuT})^*$ was also calculated from the phosphorescence band at 453 nm measurement at 77 K in glassy Me–THF to be $63.8 \pm 0.2 \text{ kcal/mol}$, which is in agreement with the E_{T_1} value evaluated by quenching of $^3(\text{PuT})^*$ within ca. 1 kcal/mol. In ethanol, a slight shift of the phosphorescence band (457 nm) was observed, suggesting that the polar character of the T₁ state is not high.

The rate constant of $^3(\text{PuT})^*$ for 1,4-cyclohexadiene (1,4-CHD; $E_{T_1} = \text{ca. } 78 \text{ kcal/mol}$)²⁸ is larger than those of *m*-terphenyl and diphenyl with lower E_{T_1} values. This indicates that H-atom abstraction from 1,4-CHD by $^3(\text{PuT})^*$ takes place.⁵ The rate constants for H-atom abstraction (k_{HT}) for 1,4-CHD evaluated in this study are similar to that reported for the xanthone triplet.⁵

Triplet Quantum Yield. The quantum yield (Φ_{T}) of $^3(\text{PuT})^*$ formation by intersystem crossing was evaluated by energy transfer from $^3(\text{PuT})^*$ to β -carotene in THF by comparison with $\Phi_{\text{T}} = 1.0$ of benzophenone (abbreviated as bp) as a standard using eq 5:^{3,30}

$$\Phi_{\text{T}}^{\text{PuT}} = \Phi_{\text{T}}^{\text{bp}} \frac{\Delta A^{\text{PuT}}}{\Delta A^{\text{bp}}} \frac{k_{\text{obs}}^{\text{PuT}}}{k_{\text{obs}}^{\text{PuT}} - k_0^{\text{PuT}}} \frac{k_{\text{obs}}^{\text{bp}} - k_0^{\text{bp}}}{k_{\text{obs}}^{\text{bp}}} \quad (5)$$

where ΔA 's are the respective maximal absorption intensities observed by the laser excitation of PuT (0.1 mM) and benzophenone (1.0 mM) and k_{obs} is the pseudo-first-order rate

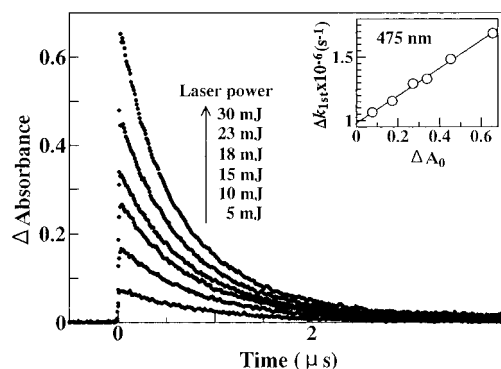
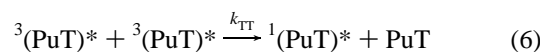


Figure 3. Laser-power dependence absorption–time profiles of $^3(\text{PuT})^*$ at 475 nm obtained by 355-nm laser photolysis of PuT (0.2 mM) in Ar-saturated THF (detector, PMT). Inset shows plot of $\Delta k_{1\text{st}}$ vs ΔA_0 .

constant for the growth of the β -carotene triplet in solutions containing benzophenone or PuT (optically matched at the excitation wavelength 355 nm). The k_0 is the rate constant for the decay of the triplet energy donors in the absence of β -carotene. The direct excitation of only the β -carotene solution did not result in any significant triplet formation because of negligible triplet yield confirmed by 355-nm laser flash photolysis.³ Thus, the Φ_{T} value in THF was evaluated to be 0.99 for $^3(\text{PuT})^*$. The k_{isc} value larger than ca. $1.3 \times 10^{10} \text{ s}^{-1}$ measured by the picosecond laser photolysis method in this study supports such a high Φ_{T} .

The triplet extinction coefficient (ϵ_{T}) of $^3(\text{PuT})^*$ was also estimated from the reported ϵ value of $^3(\text{benzophenone})^*$ as a standard ($7220 \text{ M}^{-1} \text{ cm}^{-1}$) by substituting the observed Φ_{T} and absorbance.^{3,30} The ϵ_{T} value in THF was determined to be $6100 \text{ M}^{-1} \text{ cm}^{-1}$ for $^3(\text{PuT})^*$ at 475 nm. Such a relatively large ϵ value is also characteristic of the triplet states of thiones.^{3,5}

Triplet–Triplet Annihilation. When the laser power was increased under the same concentration of PuT, the initial decay rate increased with changing decay kinetics from first order to a mixed order (first and second order) because of the triplet–triplet annihilation as shown in Figure 3 (reaction 6).



For mixed-order decay kinetics, eq 7 can be used to calculate both first- and second-order rate constants:³¹

$$\frac{-d[\ln(\Delta A_0)]}{dt} = \Delta k_{1\text{st}} = k_{1\text{st}}^0 + \frac{2k_{2\text{nd}}}{\epsilon_{\text{T}}} \Delta A_0 \quad (7)$$

where ΔA_0 is the initial absorption intensity of $^3(\text{PuT})^*$ at each laser power, $k_{2\text{nd}}$ is the T–T annihilation rate constant (k_{TT}), and $k_{1\text{st}}^0$ is the triplet-decay rate constant at low laser power. The slope of the linear plot of $\Delta k_{1\text{st}}$ vs ΔA_0 yielded $2k_{\text{TT}}/\epsilon_{\text{T}}$ (inset in Figure 3), from which the k_{TT} value was calculated to be $3.3 \times 10^9 \text{ M}^{-1} \text{ s}^{-1}$ for $^3(\text{PuT})^*$ in THF by substituting ϵ_{T} for $^3(\text{PuT})^*$ estimated above. This k_{TT} value is considerably lower than the diffusion-controlled limit ($k_{\text{d}} = 1.2 \times 10^{10} \text{ M}^{-1} \text{ s}^{-1}$ in THF), which is reasonable by taking the spin-statistical factor into consideration. At a higher laser power of 30 mJ pulse⁻¹, ca. 33% of the T–T annihilation reaction participated in the total decay of $^3(\text{PuT})^*$, while the participation of the T–T annihilation reaction is ca. 10% at 15 mJ pulse⁻¹ in THF. At a higher concentration of PuT, T–T annihilation takes place concomitant with self-quenching.

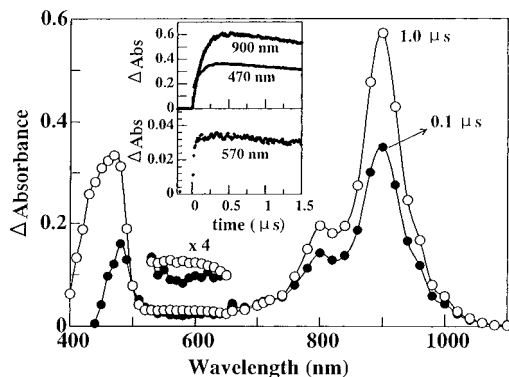


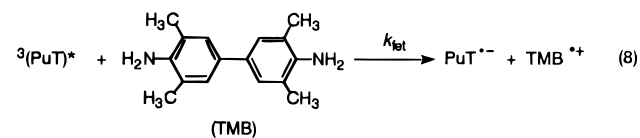
Figure 4. Transient absorption spectra in the visible and near-IR region obtained by 355-nm laser photolysis of PuT (0.1 mM) in the presence of TMB (1.0 mM) in Ar-saturated acetonitrile. Inset shows time profiles of absorption bands at 470, 570 (detector, PMT), and 900 nm (detector, Ge APD).

TABLE 3: Rate Constants for Forward Electron-Transfer Reactions (k_{fet}) and Back-Electron-Transfer Reactions (k_{bet}) in Acetonitrile^a

reactants	$k_{fet}/M^{-1} s^{-1}$ (rise) ^b	$k_{fet}/M^{-1} s^{-1}$ (decay) ^b	$k_{bet}/\epsilon/cm s^{-1} c$	$k_{bet}/M^{-1} s^{-1} c$
TMB	4.3×10^9	<i>d</i>	3.1×10^5	6.3×10^9
DNB	1.1×10^{10}	9.4×10^9	3.1×10^6	1.8×10^{10}

^a Estimation error is $\pm 5\%$. ^b Decay of $^3(PuT)^*$ at 470 nm. ^c $\epsilon_{TMB^{*+}} = 20\,200 M^{-1} cm^{-1}$ at 900 nm³³ and $\epsilon_{DNB^{*-}} = 5900 M^{-1} cm^{-1}$ at 910 nm²¹ in acetonitrile. ^d Owing to the overlap with the rise of TMB^{*+} , the k_{fet} value was not obtained from the decay.

Photoinduced Electron Transfer. The transient absorption spectra observed by the laser photolysis of PuT (0.1 mM) in the presence of TMB with 355-nm light in acetonitrile are shown in Figure 4. The transient absorption bands at 470, 800, and 900 nm are attributed to TMB^{*+} ,^{32,33} due to the electron-transfer reaction from TMB to $^3(PuT)^*$ (reaction 8). A weak band at 570 nm can be assigned to PuT^{*-} because a similar absorption band was observed by γ irradiation of PuT in Me–THF at 77 K. The rise-time profiles were observed at 470, 900, and 570 nm (inset in Figure 4). From the rise curve of TMB^{*+} at 900 nm, the first-order rate constant was evaluated by curve-fitting with a single exponential. The second-order rate constant for electron transfer (k_{fet}) can be evaluated by the TMB concentration dependence of the first-order rate constant as listed in Table 3:



At 470 nm, the rise of TMB^{*+} and decay of $^3(PuT)^*$ are overlapping. The finding that the rise-time profile was observed at 470 nm comes from the larger ϵ of TMB^{*+} compared with that of $^3(PuT)^*$ at 470 nm. Indeed, ϵ of $^3(PuT)^*$ is $6100 M^{-1} cm^{-1}$, and ϵ of TMB^{*+} is $19\,000 M^{-1} cm^{-1}$ at 470 nm.³³

In the laser flash photolysis of PuT in the presence of DNB with a light wavelength of 355 nm, the absorption band of $^3(PuT)^*$ at 470 nm disappeared within a few hundred nanoseconds, and new absorption bands appeared at 870 and 910 nm with a rising absorption–time profile in the near-IR region in acetonitrile. These absorption bands are attributed to the radical anion of DNB (DNB^{*-}).^{21,34} The first-order rate constant thus obtained from the decay profiles of $^3(PuT)^*$ by DNB is in good agreement with those obtained from the formation rise profiles

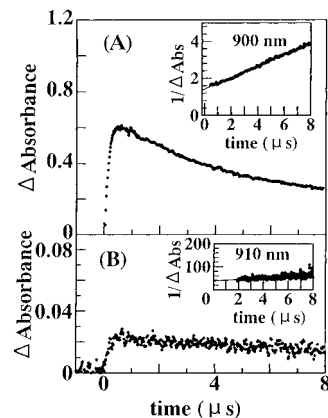
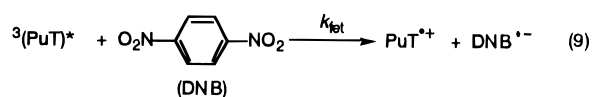


Figure 5. Absorption–time profiles (A) at 900 nm for decay of TMB^{*+} and (B) at 910 nm for the decay of DNB^{*-} obtained by 355-nm laser photolysis (detector, Ge APD) with PuT (0.1 mM) in Ar-saturated acetonitrile. Inset shows second-order plots.

of DNB^{*-} in acetonitrile. Thus, it is evident that the reaction rate constants for the quenching of $^3(PuT)^*$ by DNB and for the formation of DNB^{*-} in acetonitrile are attributed to the rate constants (k_{fet}) for electron transfer from $^3(PuT)^*$ to DNB, forming DNB^{*-} and PuT^{*+} (reaction 9):^{21,33}



The absorption intensities of the radical ions (TMB^{*+} , PuT^{*-} , and DNB^{*-}) decay slowly after the formation of the radical ions in acetonitrile. These decays obey second-order kinetics as shown in Figure 5 and can be attributed to the back-electron transfer reactions (k_{bet} in reactions 10 and 11):^{21,33}



From the slopes of the second-order plots (inset in Figure 5), the ratio of the rate constant to molar extinction coefficient ($k_{bet}^{2nd}/\epsilon_{\text{radical ion}}$) can be obtained as listed in Table 3. By substitution of the reported values of $\epsilon_{\text{radical ion}}$,^{21,33} the k_{bet}^{2nd} values were evaluated for TMB^{*+} and DNB^{*-} in acetonitrile (Table 3).

H-Atom Abstraction Reaction of $^3(PuT)^*$. In the presence of $p\text{-X}-\text{C}_6\text{H}_4\text{SH}$, formation of $p\text{-X}-\text{C}_6\text{H}_4\text{S}^{\bullet}$ ^{35–37} was observed in THF as shown in Figure 6 (Scheme 3). $^3(PuT)^*$ decreases with the rise of the absorption band of $p\text{-X}-\text{C}_6\text{H}_4\text{S}^{\bullet}$ (or α -tocopheroxy radical) due to the H-atom abstraction reaction by $^3(PuT)^*$ (inset in Figure 6). The formation of the radicals was suppressed in the presence of triplet quenchers such as O_2 , 1,3-cyclohexadiene, and phenanthrene, which suggests that the H-atom abstraction reaction occurs via $^3(PuT)^*$. The H-atom abstraction rate constants (k_{HT}) by $^3(PuT)^*$ are summarized in Table 4 with the absorption maxima of the radicals formed from the different H-atom donors.

Although the decay rate of $^3(PuT)^*$ in the presence of phenol was very slow, tocopherol is highly reactive to $^3(PuT)^*$.³⁸ For benzimidazole thiol and benzoxazole thiol, the rise-time profiles of the corresponding thio radicals were observed at 590 nm accompanied by the decay of $^3(PuT)^*$, suggesting the H-atom abstraction reaction (Scheme 4; $PuTH^{\bullet}$ denotes an H-atom adduct to PuT). On the other hand, the thio radical was not observed for benzothiazole thiol. Nevertheless, rapid decay of

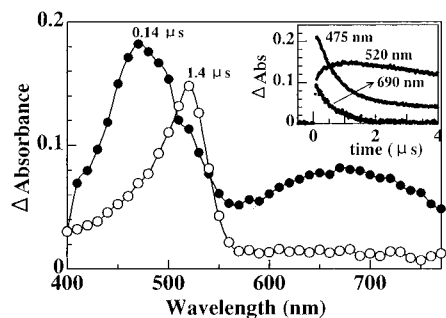


Figure 6. Transient absorption spectra observed by laser photolysis (355-nm light) of PuT (0.1 mM) with *p*-HO-C₆H₄SH (1.0 mM) in Ar-saturated THF (detector, PMT). Inset shows decay profiles of ³(PuT)* at 475 and 690 nm and rise profile of *p*-HO-C₆H₄S* at 520 nm.

SCHEME 3

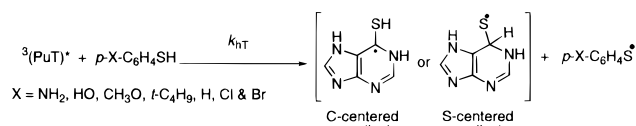
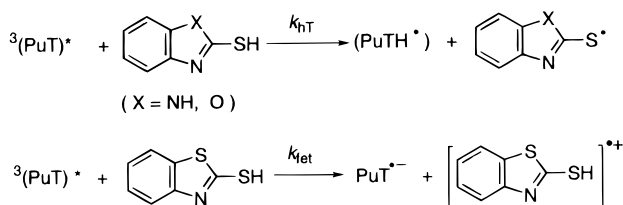


TABLE 4: Rate Constants (k_{HT}) for Hydrogen-Abstraction Reaction of ³(PuT)* with Different H-Atom Donors in THF and Hammett Parameter σ^+ of *p*-X-C₆H₄SH

H-atom donor	radical ^a	$\lambda_{\text{max}}/\text{nm}$	$k_{\text{HT}}/\text{M}^{-1} \text{s}^{-1}$ ^b	σ^+ ^c
<i>p</i> -NH ₂ -C ₆ H ₄ SH	<i>p</i> -NH ₂ -C ₆ H ₄ S*	580 ^d	1.2×10^9	-1.3
<i>p</i> -HO-C ₆ H ₄ SH	<i>p</i> -HO-C ₆ H ₄ S*	520 ^d	9.3×10^8	-0.92
<i>p</i> -CH ₃ O-C ₆ H ₄ SH	<i>p</i> -CH ₃ O-C ₆ H ₄ S*	520 ^d	6.6×10^8	-0.78
<i>p</i> - <i>tert</i> -C ₄ H ₉ -C ₆ H ₄ SH	<i>p</i> - <i>tert</i> -C ₄ H ₉ -C ₆ H ₄ S*	490 ^d	2.5×10^8	-0.26
C ₆ H ₅ SH	C ₆ H ₅ S*	480 ^d	1.9×10^8	0.0
<i>p</i> -Cl-C ₆ H ₄ SH	<i>p</i> -Cl-C ₆ H ₄ S*	510 ^d	1.0×10^8	0.11
<i>p</i> -Br-C ₆ H ₄ SH	<i>p</i> -Br-C ₆ H ₄ S*	510 ^d	1.3×10^8	0.15
α -tocopherol	α -tocopheroxy*	420 ^e	1.8×10^8	
2-MBI ^g	2-MBI* ^h	590 ^f	2.5×10^8	
2-MBO ^g	2-MBO* ^h	590 ^f	5.4×10^7	
2-MBS ^g	<i>i</i>	<i>i</i>	1.4×10^9	

^a Radical formed by the hydrogen abstraction of ³(PuT)* from different H-atom donors. ^b Estimation error is $\pm 5\%$. ^c σ^+ values are cited from ref 36. ^d References 35 and 36. ^e Reference 38. ^f Reference 37. ^g 2-MBI, 2-mercaptobenzimidazole; 2-MBO, 2-mercaptobenzoxazole; 2-MBS, 2-mercaptobenzothiazole. ^h 2-MBI*, benzimidazole-2-thio radical; 2-MBO*, benzoxazole-2-thio radical. ⁱ Benzothiazol-2-thio radical at 590 nm was not observed.

SCHEME 4



³(PuT)* was observed, suggesting the electron-transfer reaction between ³(PuT)* and benzothiazole thiol (Scheme 4).

To investigate the substituent effect for the reactions of ³(PuT)* with *p*-X-C₆H₄SH as the H-atom donors, a Hammett plot of $\log k_{\text{HT}}$ vs σ^+ constants of *p*-X-C₆H₄SH is shown in Figure 7. A negative slope ($\rho^+ = \text{ca. } -1.0$) of the Hammett relation (eq 12)³⁶ implies a strong electrophilicity of ³(PuT)* with respect to H-S in *p*-X-C₆H₄SH.^{35,36}

$$\Delta(\log k_{\text{HT}}) = \rho^+ \sigma^+_{\text{X}} \quad (12)$$

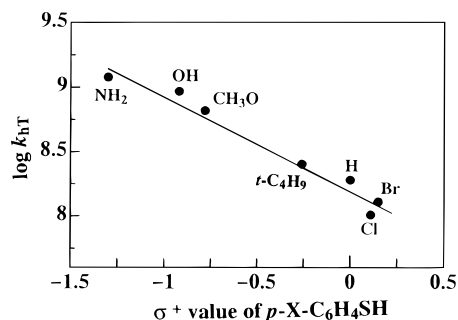


Figure 7. Hammett plot of $\log k_{\text{HT}}$ vs σ^+ constants of *p*-X-C₆H₄SH for reaction with ³(PuT)* in Ar-saturated THF.

TABLE 5: Addition-Reaction Rate Constants (k_{ad}), $\log k_{\text{ad}}$, and Alfrey-Price's e Values of Alkenes for Reaction with ³(PuT)* in THF

alkenes		$k_{\text{ad}}/\text{M}^{-1} \text{s}^{-1}$ ^a	e value ^b
CH ₂ =C(CH ₃)Ph	(α -MSt)	2.0×10^9	-0.81
CH ₂ =C(CH ₃)CO ₂ CH ₃	(MMA)	7.3×10^8	+0.40
CH ₂ =C(CH ₃)CN	(MAN)	7.6×10^8	+0.61
CH ₂ =CHCN	(AN)	4.8×10^8	+1.20
CH ₂ =CHOBu	(BVE)	2.4×10^8	-1.77
CH ₂ =CHOEt	(EVE)	2.7×10^8	-1.17
CH ₂ =CHOCOCH ₃	(VAc)	1.3×10^8	-0.22

^a Estimation error is $\pm 5\%$. ^b e values of alkenes are cited from ref 36.

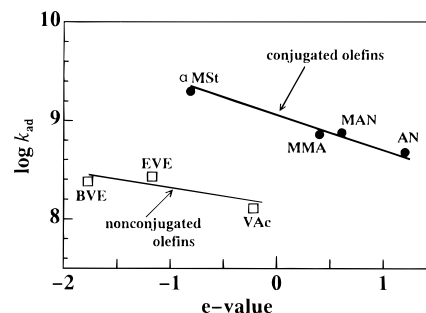


Figure 8. Plots of $\log k_{\text{ad}}$ for ³(PuT)* vs Alfrey-Price's e values of different alkenes in Ar-saturated THF.

The electrophilic nature of ³(PuT)* suggesting that sulfur is the active site for the reaction of ³(PuT)* is similar to that of the aromatic and aliphatic thio radicals.^{36,39} Thus, this observation suggested that the C-centered radical (Scheme 3) was formed first by H-atom abstraction of ³(PuT)*.

Addition Reaction to Alkenes. On addition of alkenes, the decay rate of ³(PuT)* increases with increasing concentration of alkenes because of the reaction with ³(PuT)*. The cycloaddition reaction is most probable, like for other aromatic thiones.^{8,39} The values of the addition reaction rate constants (k_{ad}) for several alkenes are summarized in Table 5 with Alfrey-Price's e values,³⁶ which are a measure of the polar nature of C=C. The k_{ad} values are plotted vs e values as shown in Figure 8. Conjugated are more reactive than nonconjugated alkenes toward ³(PuT)*. Conjugated alkenes substituted by electron-donating groups such as α -methylstyrene are more reactive than those substituted by electron-withdrawing groups such as CH₂=CHCN.

The plots can be divided into two groups according to the conjugative abilities of vinyl monomers. Conjugative ability seems to be a main factor for determining reactivity of alkenes to ³(PuT)*. In each group, the slope is a measure of the polar character of the attacking ³(PuT)*. Negative slopes suggest the electrophilicity of ³(PuT)* with respect to C=C.^{36,39} This is

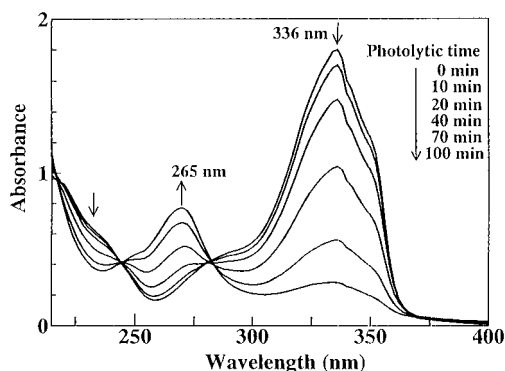


Figure 9. Steady-state absorption spectra observed by photolysis of PuT (0.1 mM) in Ar-saturated THF with light of wavelength longer than 310 nm at room temperature. The 265-nm band is due to purine.

the same trend for the electrophilic thio radicals.^{35,36,39} The electrophilic nature of $^3(\text{PuT})^*$ indicates that a partial charge transfer is generated in the transition state during the addition of $^3(\text{PuT})^*$ toward alkenes such as the triplet state of xanthione.³⁹ Thus, the initial bond formation with alkenes would be expected to occur between the C atom in C=C and the S atom in $^3(\text{PuT})^*$.^{8,39}

Steady-Light Photolysis. Photochemical changes of PuT caused by steady-light (>310 nm) illumination were studied. By the steady photolysis of PuT (Figure 9), the thione band at 336 nm decreases slowly with irradiation time ($t_{1/2} = 45$ min in Ar-saturated THF) accompanied by an appearance of a new band at 265 nm, which is assigned to purine as described in the experimental part.^{17,40} It was confirmed that the H-atom donor solvents (i.e., in 2-PrOH; $t_{1/2} = 20$ min) or additives [i.e., 1,4-CHD (10 mM); $t_{1/2} = 18$ min] are indispensable for the desulfurization reaction of PuT, since only a small UV spectral change was observed in poor H-atom donor solvents such as acetonitrile by photoillumination even for 2 h. For the steady-state photolysis of PuT in THF, the quantum yield of desulfurization was evaluated to be 0.11 by the actinometric method.¹⁸ On addition of triplet quenchers such as 1,3-CHD and isoprene, the desulfurization reaction did not take place, suggesting that $^3(\text{PuT})^*$ is the precursor of the photodesulfurization reaction of PuT in the presence of H-atom donors.

Character of T_1 . The observed energy gap between S_2 [85 kcal/mol with (π, π^*) character] and S_1 [ca. 66 kcal/mol with (n, π^*) character] is as large as 19 kcal/mol (7000 cm^{-1}). On this basis, it is presumed that T_1 has $^3(n, \pi^*)$ character by an empirical rule.^{1,4,10,41} Small $S_1 - T_1$ gap less than ca. 3 kcal/mol (ca. 1000 cm^{-1}) also supports the $^3(n, \pi^*)$ character.¹ The high reactivity and electrophilicity of $^3(\text{PuT})^*$ correspond to the $^3(n, \pi^*)$ character of the T_1 state from the analogy of the C=O triplet state. On the other hand, the nonpolar nature of the T_1 state evaluated from the shift of the phosphorescence data suggests $^3(\pi, \pi^*)$ character. The MO calculation of $^3(\text{PuT})^*$ by the MNDO method⁴² employing the restricted open-shell Hartree-Fock method with configuration interactions suggests that both the upper and lower SOMO's have π character. Thus, it is difficult to determine definitively the character of T_1 . Probably, the T_1 of PuT has a mixed character of $^3(n, \pi^*)$ and $^3(\pi, \pi^*)$ as observed for other thiones.¹⁰

Summary

The importance of $^3(\text{PuT})^*$ in photophysical and photochemical processes was proved by laser flash photolysis methods. The high Φ_T value, a short intrinsic triplet lifetime, and a high self-quenching rate are similar to the properties of the thiones without

nitrogen atoms. The lowest triplet-state energy ($E_{T_1} = 63$ kcal) is relatively high, which is the origin of efficient electron-transfer ability of $^3(\text{PuT})^*$. Therefore, $^3(\text{PuT})^*$ acts as both electron donor and acceptor. The electrophilic character of $^3(\text{PuT})^*$ was revealed by the substituent effects in H-atom abstraction and addition reactions. The high electrophilicity of $^3(\text{PuT})^*$ implies that the S atom is the reactive center. The T_1 of PuT may have a mixed character of $^3(n, \pi^*)$ and $^3(\pi, \pi^*)$.

Acknowledgment. The present work was partly supported by a Grant-in-Aid on Priority-Area-Research on "Carbon Alloys" (No. 09243201) from the Ministry of Education, Science, Sports and Culture. The authors express thanks to Takeda Science Foundation and to Professor H. Hiratsuka of Gunma University.

References and Notes

- Wirz, J. J. *Chem. Soc., Perkin Trans. 2* **1973**, 1307.
- de Mayo, P. *Acc. Chem. Res.* **1976**, *9*, 52.
- Kumar, C. V.; Qin, L.; Das, P. K. *J. Chem. Soc., Faraday Trans. 2* **1984**, *80*, 783.
- Maciejewski, A.; Demmer, D. R.; James, D. R.; Safarzadeh-Amiri, A.; Verrall, R. E.; Steer, R. P. *J. Am. Chem. Soc.* **1985**, *107*, 2831.
- Bhattachayya, K.; Ramamurthy, V.; Das, P. K. *J. Phys. Chem.* **1987**, *91*, 5626.
- Maciejewski, A.; Syzanski, M.; Steer, R. P. *J. Phys. Chem.* **1988**, *92*, 6939.
- Minto, R.; Samanta, A.; Das, P. K. *Can. J. Chem.* **1989**, *67*, 967.
- Kamphuis, J.; Bos, H. J. T.; Visser, R. J.; Huizer, B. H.; Varma, C. A. G. O. *J. Chem. Soc., Perkin Trans. 2* **1986**, 1867.
- Ramamurthy, V.; Steer, R. P. *Acc. Chem. Res.* **1988**, *21*, 380.
- (a) Maciejewski, A.; Steer, R. P. *Chem. Rev. (Washington, D.C.)* **1993**, *93*, 67. (b) Lapinski, L.; Prusinowska, D.; Nowak, M. J.; Bretner, M.; Felczak, F.; Maes, G.; Adamowicz, L. *Spectrochim. Acta, Part A* **1996**, *52*, 645.
- (a) Barton, D. H. C.; Crich, D.; Motherwell, W. B. *Tetrahedron* **1985**, *41*, 3901. (b) Barton, D. H. C.; Zard, S. Z. *Pure Appl. Chem.* **1986**, *58*, 675. (c) Barton, D. H. C.; Jaszberenyi, J. Cs.; Morrell, A. I. *Tetrahedron Lett.* **1991**, *32*, 311.
- (a) Newcomb, M.; Park, U. *J. Am. Chem. Soc.* **1986**, *108*, 4132. (b) Newcomb, M.; Kaplan, J. *Tetrahedron Lett.* **1987**, *28*, 1615.
- Calabresi, P.; Parks, R. E., Jr. *The Pharmacological Basis of Therapeutics*, 4th ed.; Goodman, L. S., Gilman, A., Eds.; Macmillan: New York, 1970; p 1371.
- Hyslop, R. M.; Jardine, I. *J. Pharmacol. Exp. Ther.* **1981**, *218*, 621.
- Hemmens, V. J.; Moore, D. E. *Photochem. Photobiol.* **1986**, *43*, 247.
- Hemmens, V. J.; Moore, D. E. *J. Chem. Soc., Perkin Trans. 2* **1984**, 209.
- Murov, S. L. *Handbook of Photochemistry*; Marcel Dekker: New York, 1973; pp 119–122.
- Watanabe, A.; Ito, O. *J. Phys. Chem.* **1994**, *98*, 7736.
- Alam, M. M.; Watanabe, A.; Ito, O. *J. Org. Chem.* **1995**, *60*, 3440.
- Watanabe, A.; Ito, O.; Watanabe, M.; Saito, H.; Koishi, M. *J. Phys. Chem.* **1996**, *100*, 10518.
- Fujitsuka, M.; Sato, T.; Shimidzu, T.; Watanabe, A.; Ito, O. *J. Phys. Chem. A* **1997**, *101*, 1056.
- Al-Mosawi, A. L.; Miller, J. N. *Analyst* **1980**, *105*, 448.
- (a) Arai, S.; Dorfman, L. M. *J. Chem. Phys.* **1964**, *41*, 2190. (b) Gould, R. F. *Solvated Electron*; Advances in Chemistry Series 50; American Chemical Society: Washington, DC, 1965; Chapter 4, p 41.
- Wasserman, H. H.; Murray, R. W. In *Singlet Oxygen*; Academic Press: New York, 1979; Chapters 5, 6, 8, and 9.
- Lambert, C.; Redmond, R. W. *Chem. Phys. Lett.* **1994**, *228*, 495.
- Farmilo, A.; Wilkinson, F. *Chem. Phys. Lett.* **1975**, *34*, 575.
- Murov, S. I. *Handbook of Photochemistry*; Marcel Dekker: New York, 1973.
- Evaluated from T_1 of 2-butene.²⁷
- Sandros, K. *Acta Chem. Scand.* **1964**, *18*, 2355.
- Lamola, A. A.; Hammond, G. S. *J. Chem. Phys.* **1965**, *43*, 2129.
- Zwicker, E. F.; Grossweiner, L. I. *J. Phys. Chem.* **1963**, *67*, 549.
- Watanabe, A.; Ito, O.; Mori, K. *Synth. Met.* **1989**, *32*, 237.
- Sasaki, Y.; Yoshikawa, Y.; Watanabe, A.; Ito, O. *J. Chem. Soc., Faraday Trans.* **1995**, *91*, 2287.
- Shida, T. *Electronic Absorption Spectra of Radical Ions*; Physical Science Data 34; Elsevier: Amsterdam, 1988.

(35) (a) Ito, O.; Matsuda, M. *J. Am. Chem. Soc.* **1979**, *101*, 1815. (b) Ito, O.; Matsuda, M. *J. Am. Chem. Soc.* **1979**, *101*, 5732. (c) Ito, O.; Matsuda, M. *J. Am. Chem. Soc.* **1982**, *104*, 1815.

(36) (a) Ito, O. *Res. Chem. Intermed.* **1995**, *21* (1), 69. (b) Yoshizawa, H.; Ito, O.; Matsuda, M. *Br. Polym. J.* **1988**, *20*, 441.

(37) (a) Alam, M. M.; Konami, H.; Watanabe, A.; Ito, O. *J. Chem. Soc., Perkin Trans. 2* **1996**, 263. (b) Dey, G. R.; Naik, D. B.; Kishore, K.; Moorthy, P. N. *Res. Chem. Intermed.* **1995**, *21* (1), 47.

(38) Bohm, F.; Edge, R.; Land, E. J.; McGarvey, D. J.; Truscott, T. G. *J. Am. Chem. Soc.* **1997**, *119*, 621.

(39) Turro, N. J.; Ramamurthy, V. *Tetrahedron Lett.* **1976**, *28*, 2423.

(40) UV-spectrum of Purine. *UV Atlas of Organic Compounds*; Butterworths: London, 1968; Vol. IV.

(41) El Sayed, M. A. *J. Chem. Phys.* **1963**, *38*, 2834.

(42) (a) Stewart, J. J. P. *J. Comput. Chem.* **1989**, *10*, 209. (b) Stewart, J. J. P. *QCPE Bull.* **1989**, *9*, 10.